Single Pulse, Single Crystal Laser-Induced Nucleation of Potassium Chloride

Cite as:
Alexander, A. J., & Camp, P. J. (2009). Single Pulse, Single Crystal Laser-Induced Nucleation of Potassium Chloride. *Crystal Growth & Design*, 9(2), 958-963.

Manuscript received: 10/07/2008; Accepted: 29/09/2008; Article published: 04/12/2008

Single Pulse, Single Crystal Laser-Induced Nucleation of Potassium Chloride**

Andrew J. Alexander* and Philip J. Camp

School of Chemistry, Joseph Black Building, University of Edinburgh, West Mains Road, Edinburgh, EH9 3JJ, UK.

[*]Corresponding author; e-mail: andrew.alexander@ed.ac.uk; tel: +44 131 650 4741; fax: +44 131 650 4743.

[**]A.J.A thanks the Royal Society for a University Research Fellowship. The authors thank Professors Paul Madden and Daan Frenkel for useful discussions.

Graphical abstract:

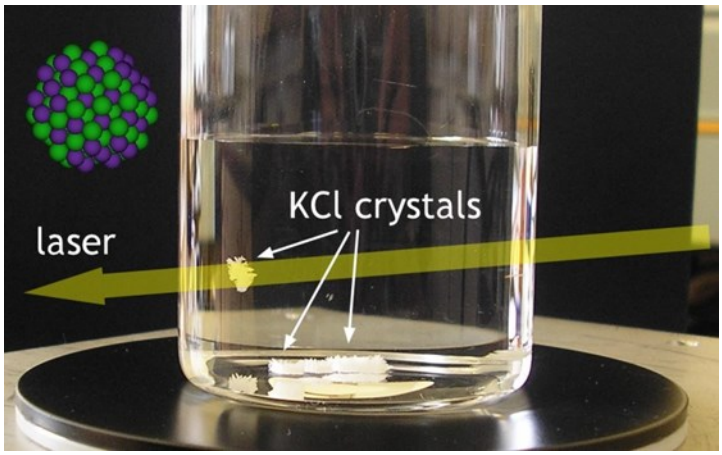

Summary:
We report an experimental study of laser-induced nucleation in supersaturated aqueous solutions of potassium chloride. The dependences of nucleation on laser-pulse power (above a minimum threshold) and degree of supersaturation have been measured. These dependences are well described by classical nucleation theory, adapted to include dielectric effects arising from the interaction between crystal nuclei and the laser electric field.

Abstract

The non-photochemical laser-induced nucleation of aqueous supersaturated solutions of potassium chloride is demonstrated. We have observed that a single, 7 ns pulse of near-infrared (1064 nm) laser light can be used to grow a single crystal of potassium chloride. The experimental results are analyzed using a model in which nucleation is enhanced through the isotropic electronic polarization of sub-critical crystal nuclei by the laser radiation, and the associated reduction in free-energy of the nuclei. Classical nucleation theory is used to calculate the fraction of sub-critical nuclei, initially in zero field, which become supercritical in the laser field; this fraction is correlated with the crystallization yield, and is shown to describe successfully the dependences of the experimentally observed yields upon laser-power and supersaturation. The experimental results are analyzed to obtain a phenomenological value of the crystal–solution interfacial tension $\gamma = 2.19 \pm 0.03 \text{ mJ m}^{-2}$.

1. Introduction

Photochemically induced nucleation has been known since the early work of John Tyndall in 1869,[1] and has been studied in a range of vapors and solutions.[2-4] In photochemically induced nucleation, the light has sufficient energy per photon to cause ionization, or to create radicals that subsequently react to produce nucleation centers. By contrast, non-photochemical laser-induced nucleation (NPLIN) was discovered by Garetz *et al.* in 1996.[5] In their work, Garetz *et al.* shot multiple pulses (20 ns-width pulses, with energy $\sim 0.1 \text{ J pulse}^{-1}$) of near-infrared ($1064 \text{ nm}$) laser light at supersaturated aqueous solutions of urea. The wavelength and power of the light were deemed not capable of inducing photochemistry, and if anything the laser radiation was more likely to inhibit crystallization by heating the solvent. Having observed that the crystallites so formed were aligned preferentially along the linear axis of polarization of the pulsed light, Garetz *et al.* explained their results in terms of a nonlinear optical Kerr-type mechanism.[6] The molecules are believed to be randomly aligned in sub-critical nuclei, and the nuclei become critical when molecules are aligned by the intense peak electric field of the laser light, which interacts with the polarizability anisotropy of the molecules.[7]

Following on from their initial discovery, Garetz and co-workers have observed similar effects in a range of molecules, most notably glycine, for which they observed the remarkable result that the α and γ polymorphs were induced to crystallize from aqueous solution by circular or linear polarizations of the incident laser light, respectively, termed *polarization switching*.[7,8] Over the range of superaturations studied, α-glycine is always produced by spontaneous nucleation, although γ-glycine is the thermodynamically more stable polymorph.[9] Polarization switching has also recently been reported for l-histidine.[10] For both glycine and l-histidine, it was found that there is a definite window

of supersaturation and temperature conditions where the effect is observed.[10,11] Polarization switching can be correlated with matching between the shapes of the polarizability anisotropies for solute dimers and oligomers and the packing arrangements of molecules in different polymorphs. For example, α-glycine is composed of double planes of cyclic dimers (disc-like polarizability) and γ-glycine is composed of helical chains (rod-like polarizability).[7] The linear or circular polarization of the light can cause different degrees of alignment according to the shape of the polarizability anisotropy. Although the NPLIN results can be explained qualitatively in terms of polarizability anisotropy, Garetz *et al.* point out that the interaction energy between the incident light and a single glycine molecule is only $\sim 10^{-4} k_B T$, and suggest that the field operates cooperatively on clusters of glycine molecules, for which the polarizability effect scales with the number of molecules.[7]

Yoshikawa *et al.* studied the laser-induced nucleation of supersaturated aqueous solutions of urea using a focused Ti^{3+}:sapphire laser producing $120\,fs$ pulses of $800\,nm$ radiation.[12] Here, not only was the beam focused, but the sample was bombarded with $50-300\,\mu J$ pulses at $1\,kHz$. The peak power densities in these experiments were significantly higher than in the work by Garetz *et al*. since the energy of the pulse is delivered over a shorter time and at the focus of the beam; in comparison, the experiments of Garetz *et al*. used unfocussed $20\,ns$ pulses. Femtosecond pulses are capable of causing multiphoton excitation, leading to cavitation and shock-wave formation in the solution,[13] and are also likely to cause ionization. Therefore, the results of Yoshikawa *et al.* should not be compared directly with the NPLIN effects observed in the experiments of Garetz *et al*.

A recent report by Sugiyama *et al.* considers the non-photochemical nucleation of glycine, but using a focused continuous-wave laser.[14] The $Nd^{3+}:YVO_4$ beam was focused onto the air–liquid interface of a droplet of supersaturated glycine in D_2O by a microscope objective. After several seconds of irradiation, small crystals of glycine were observed in the region of the beam, and the authors attribute this to the trapping potential of the focused beam causing aggregation of sub-critical clusters. This is quite likely to be a different mechanism from the NPLIN observed by Garetz *et al*., since the peak power density of the electric field will be orders of magnitude lower than in the nanosecond laser pulses. The focusing of the beam at the vapor-liquid interface is likely to cause local heating and evaporation, enhancing the local supersaturation.

A number of studies demonstrating enhanced rates of crystallization in the presence of a DC electric field have also been published.[15] There have been very few quantitative studies of the effect, although models based on the interaction of the electric field with the dielectric have been developed.[16-18] In many cases, however, the importance of other effects, such as enhanced convection or evaporation due to heating, is not accounted for.[19,20] In an extension of their work on glycine, Garetz and co-

workers showed that a strong DC field of $6\times10^{5}\ \mathrm{V\,m^{-1}}$ induced nucleation of γ-glycine, and highlighted this as further evidence to support the operation of a Kerr-type mechanism for NPLIN.[21]

In the present work, we demonstrate NPLIN in supersaturated aqueous solutions of potassium chloride. In contrast to the non-linear optical Kerr-type mechanism described by Garetz *et al*., the most likely mechanism is shown to be due to the *isotropic* electronic polarizability of clusters of KCl, and we develop a model based on classical nucleation theory that is able to account quantitatively for the experimental results obtained.

2. Experimental methods

Samples were made by dissolving KCl (Fluka, puriss > 99%) in de-ionized water (Fisher, HPLC grade). One set of samples was also made using highly purified KCl (Merck, 99.999%) in fresh ultrapure water (resistivity $18.2\ \mathrm{M\Omega\text{-}cm}$). Solutions were dissolved and filtered while hot through disposable syringe filters ($0.2\ \mu\mathrm{m}$, Minisart) into screw-cap glass vials (volume $4\ \mathrm{cm^3}$, diameter 20 mm). Great care was taken to work in an environment free from dust: in the case of the highly purified reagents, the samples were prepared in an enclosed hood under a positive pressure of argon gas. The saturation concentration of KCl in aqueous solution at $23\,^{\circ}\mathrm{C}$ (c_S^{23}) is $34.95\ \mathrm{g}$ per $100\ \mathrm{g}$ of $\mathrm{H_2O}$. Supersaturations (S) in the range $1.053 \le S = c/c_S^{23} \le 1.102$ were studied; approximately 30 sample vials were prepared for each concentration. Once tightly sealed, the vials can be re-heated and ultrasonicated to dissolve the KCl, followed by slow cooling. Compared to previous reports,[5,7,8,11,21,22] significant periods (days) of ageing of the supersaturated solution were not required, and the samples were used approximately 30 minutes after cooling to the target temperature of $23\,^{\circ}\mathrm{C}$.

Nucleation was induced by placing the vials in the path of a near-infrared (NIR) laser beam, taking care to ensure that the beam ($5.8\ \mathrm{mm}$ diameter) passed through the center of the solution. The light used was the fundamental of a Q-switched $\mathrm{Nd^{3+}:YAG}$ laser (Continuum, Surelite II-10), which produces $7\ \mathrm{ns}$ pulses of $1064\ \mathrm{nm}$ light. The beam was linearly polarized using a Glan-laser polarizer (Optics for Research); when required, circular polarization was produced by a zero-order quartz quarter-wave plate (Coherent). The average laser power as measured by a power meter (Ophir) was converted to a peak power density, taking into account the minor refraction due to the shape of the sample vial. The volume of sample irradiated was calculated to be 0.39 $\mathrm{cm^3}$.

For a particular concentration and given laser power, each sample vial was taken from a temperature-controlled water bath and shot with a *single* laser pulse. After ca. 20 mins, all the vials were checked,

and the total number of samples showing crystals were counted and removed from the batch; the remaining samples were then shot at an increased laser power, and so on. Each experiment gives a cumulative number of samples crystallized at a given laser power, similar to those reported by Matic *et al.*:[22] the assumption is that all samples which nucleated below a given laser power would have nucleated if shot at that laser power. We verified that this cumulative method of determining the fraction of samples nucleated was the same as shooting all samples at any given fixed power level.

Significantly, we have noted that a *single* laser shot yielded on average a *single* crystal of KCl. At higher laser powers, we observed an increased occurrence of more than one crystal per single laser shot (as many as 4 at the higher concentrations). By contrast, previous experiments on NPLIN have required multiple (tens to hundreds, or more) of laser pulses, and yielded a multitude of crystals.

3. Results

Plots of the cumulative fraction of samples that crystallized versus peak power density are shown in Fig. 1. The results appear to show a threshold power below which solutions do not crystallize. One or two samples were found to have crystallized at lower powers, but these are believed to be due to other factors, such as mechanical shock during manual handling of the samples. It was observed that the samples could be shot multiple times at powers below the threshold without crystallization, supporting the existence of a definite threshold. The plots also show an apparently linear dependence of probability of nucleation on laser power. The data have been fitted by straight lines for each supersaturation, and the resulting power threshold and laser-power dependence are shown in Figs. 2a and 2b, respectively. For the laser-power dependence, the slope of the plot is a measure of how labile the samples are to nucleation at a given supersaturation; we will refer to the magnitude of this slope as the *lability* of the samples. The mean threshold peak-power density was found to be $6.4 \pm 0.5\,\mathrm{MW\,cm^{-2}}$ ($6.4\,\mathrm{mJ\,pulse^{-1}}$ delivered in the 5.8 mm diameter beam) which is significantly lower than the thresholds observed by Garetz *et al.* for urea ($20\text{-}60\,\mathrm{MW\,cm^{-2}}$).[5,22] Also shown in Fig. 2 are the results obtained using the ultrapure reagents, which are very close within uncertainties to the other results. The ultrapure samples appear to be fractionally less labile: possible reasons for this may be that there are fewer chemical impurities (sodium is the most common impurity in KCl), or fewer physical impurities (i.e., 'dust') in the ultrapure samples.

We have carried out some preliminary studies to rule out the effects of the walls of the vessel. It was found that the threshold for nucleation was not changed for polyvinylpyrrolidone (PVP) vessels compared to borosilicate glass. We also observed that the location of nucleation in the beam path of the laser through the solution was random.

To test the effect of residual dust in the sample vials, we set up a glass tube ($5.5\,\mathrm{mm}$ diameter) which was first washed with concentrated nitric acid and rinsed extensively with ultrapure water. By then passing several cm^3 of hot, $0.2\,\mu\mathrm{m}$-filtered KCl solution through the tube, we expect to remove any other residual dust (> 200 nm) remaining after washing. After this purging process, the portion of solution in the tube was allowed to cool to $23\,^{\circ}\mathrm{C}$ (296.15 K), thus becoming supersaturated, and was shot with a single laser pulse ($20\,\mathrm{MW\,cm^{-2}}$) as described above. We found that, within a short time, one or more small crystallites were visible, and these started to grow and fall out of solution. The sample could be refreshed by flowing more hot solution through the tube. By repeating the above process many times, we also verified our determination of the nucleation power threshold, as given above. We believe that physical impurities (> 200 nm) are not necessary to cause the laser-induced nucleation in this system. We observe, however, that solutions that were not filtered during the preparation outlined above are significantly more labile to nucleation, suggesting that dust can promote laser-induced nucleation.

The dependence of nucleation on polarization of the laser light was tested by shooting samples at supersaturation $S = 1.060$ with linearly (LPL) and circularly (CPL) polarized light at $15\,\mathrm{MW\,cm^{-2}}$ peak power. The results are shown in Fig. 3, compared to the power-dependent results at the same supersaturation. No dependence on polarization was observed.

4. Classical nucleation theory

Garetz *et al.* have demonstrated NPLIN for a number of molecules in supersaturated aqueous solutions, such as urea and glycine.[5,8] For the present system we note two key experimental observations that are different from their work:

(1) significant periods (hours or days) of ageing of the supersaturated solutions are not required;

(2) nucleation of a single crystal of KCl can be induced with a single laser pulse, whereas urea and glycine required hundreds of shots over tens of seconds.[22]

These practical issues make the NPLIN effect significantly easier to quantify, as we shall develop in the following discussion.

At first sight, one would be tempted to look at the strong electric-dipole moments of urea and glycine as the cause of the nucleation. Because of the frequency of the alternating electric field in the NIR–visible light, however, Garetz *et al*. pointed out that the light must induce an electronic polarization in

the molecules[5,8] and suggested that the polarization *anisotropy* of the molecules cause them to become aligned to the electric field of the light. This interaction is well-known as the nonlinear optical Kerr-effect, and the nominal picosecond timescale for molecular re-orientation is compatible with the nanosecond timescale of the laser pulses.[6]

As discussed in the Introduction, the evidence for the Kerr-effect mechanism is very strong, in particular from observations of the effects of the *polarization* of the light. For example, it was observed that the initially formed crystallites of urea are aligned to the linear polarization of the laser beam.[5] It has also been shown that (in a window of temperature and supersaturation conditions[11]) α-glycine is induced by circularly polarized light and γ-glycine is induced by linearly polarized light.[7]

In the present work, we rule out the Kerr effect for the following reasons. First, KCl crystallizes into a cubic rock-salt structure: there are, as such, no molecules to be aligned in the manner envisaged for the Kerr effect. Second, we observe no polarization dependence in the nucleation (see Fig. 3), and there is no preferred polarization axis in the crystal structure. We believe that the likely mechanism involves electronic polarization of sub-critical KCl clusters by the electric field of the light. It is well known that the free energy of an isotropic and homogeneous dielectric particle with dielectric constant ε_p immersed in a medium of dielectric constant ε_s is lowered in the presence of a static electric field provided that $\varepsilon_p > \varepsilon_s$. The relationship between ε_p and the atomic polarizability may follow a relation of the Clausius-Mossotti type, within the usual approximations.[23] This change in free energy arising from dielectric effects, $\Delta W(E)$, has been calculated to be[18,24]

$$\Delta W(E) = -aV_p E^2 \qquad (1)$$

where

$$a = \frac{3\varepsilon_0 \varepsilon_s}{2}\left(\frac{\varepsilon_p - \varepsilon_s}{\varepsilon_p + 2\varepsilon_s}\right), \qquad (2)$$

E is the electric field strength, V_p is the volume of the particle, and ε_0 is the vacuum dielectric permittivity. From the Maxwell relation $\varepsilon = n^2$ and the refractive indices at $1064\,\mathrm{nm}$, we obtain for KCl $\varepsilon_p = 2.1897$ and for water $\varepsilon_s = 1.7535$.[25] We thereby calculate $a = 1.7832\times10^{-12}\ \mathrm{F\,m^{-1}}$. The frequency of the laser radiation ($3\times10^{14}\,\mathrm{Hz}$) is much less than the optical resonance frequency for electronic polarization[23] and significantly greater than the frequency of rotation for a cluster. (As an example, for a $1\,\mathrm{nm}$ spherical particle in water at ambient temperature, the Brownian rotation time

is $\tau_B = 3V_p\eta/k_BT = 4\times10^{-10}$ s where $\eta = 10^{-3}$ Pa s is the viscosity of the carrier liquid.[26]) Under these conditions, and assuming that the clusters are dielectrically homogeneous and isotropic, during a 7 ns laser pulse the electronic polarization can be considered as an instantaneous response to the electric field, even at the peak intensity of the pulse. In simple terms, the electronic polarization is able to 'follow the field', without a phase lag or dielectric loss. The electric field strength can be obtained from the energy flux density of the light given by

$$I = \frac{1}{2}c\varepsilon_0 E^2 \quad (3)$$

where *c* is the speed of light. The observed threshold peak power density $I = 6.4$ MW cm^{-2} corresponds to a peak electric field of $E = 6.9\times10^6$ V m^{-1}. In classical nucleation theory the free energy change $\Delta G(r,0)$ on forming a spherical cluster of radius *r* in the absence of an external electric field can be written[27]

$$\Delta G(r,0) = 4\pi r^2\gamma - \frac{4}{3}\pi r^3 A\ln S \quad (4)$$

where γ is the solution-crystal interfacial tension, $A = \rho RT/M$ where ρ is the mass density, *M* is the molar mass of the solid (which for KCl have values of 1.984 g cm^{-3} and 74.551 g mol^{-1}, respectively[25]), *S* is the supersaturation (see Experimental Methods section), and $k_BT\ln S = \mu(\text{solution}) - \mu(\text{crystal})$ is the difference in chemical potentials of KCl in the crystal and in solution. In an applied field the free energy is supplemented by the electrostatic free energy given in Eq. (1), and can therefore be written

$$\Delta G(r,E) = 4\pi r^2\gamma - \frac{4}{3}\pi r^3\left(A\ln S + aE^2\right). \quad (5)$$

Eq. (5) predicts that the free-energy barrier to nucleation is located at a critical cluster radius $r_c(E)$ given by

$$r_c(E) = \frac{2\gamma}{A\ln S + aE^2}. \quad (6)$$

It is clear from Eq. (6) that the presence of the field lowers the critical cluster radius, and hence any clusters with radii $r > r_c(E)$ should fall on to the supercritical portion of the modified free-energy

curve [Eq. (5)] and hence nucleate. This is shown schematically in Fig. 4. To model the power and supersaturation dependence of the laser-induced nucleation, we therefore calculate the fraction of samples that would become critical through the application of an applied electric field, i.e., the proportion of subcritical clusters in zero field with radii in the range $r_c(E) \le r \le r_c(0)$. The probability distribution of the cluster radius in zero field is proportional to $\exp\left[-\Delta G(r,0)/k_B T\right]$ and so the required fraction is

$$f = \left\{ \int_{r_c(E)}^{r_c(0)} \exp\left[-\Delta G(r,0)/k_B T\right] \mathrm{d}r \right\} \left\{ \int_{0}^{r_c(0)} \exp\left[-\Delta G(r,0)/k_B T\right] \mathrm{d}r \right\}^{-1} \quad (7)$$

Eq. (7) can be evaluated conveniently by numerical integration using $\Delta G(r,0)$ given in Eq. (4). In Fig. 5 we plot the lability to nucleation versus the supersaturation of the KCl solution taken from Fig. 2b, onto which we have plotted results from the model Eq. (7). It is found that the linear portion of the experimental data can only be reproduced by the model for particular values of the interfacial energy γ, and by including an empirical scaling factor k. The model [Eq.(7)] gives the dimensionless fraction of clusters that become critical in the presence of the field, but not the absolute concentrations of clusters irradiated. In other words, the experimental data (Fig. 1) incorporate an implicit volume factor: increasing the volume of sample irradiated would increase the number of nucleation events. The model fractions are therefore multiplied by the empirical scaling factor k before comparing them to the experimental fractions. The experimentally measured lability as a function of supersaturation has been fitted with the prediction of Eq. (7) using a nonlinear least-squares method to obtain the best-fit values $\gamma = 2.19 \pm 0.03$ mJ m^{-2} and $k = (7.78 \pm 0.12) \times 10^4$; the resulting curve is shown as the solid line in Fig. 5. Also plotted in Fig. 5 are model values obtained with the same empirical scaling factor k, but with different values of γ, showing how the supersaturation dependence of the lability varies with γ.

The observed power dependences for KCl, shown in Fig. 1, are approximately linear, compared to the non-linear dependences observed for urea by Matic *et al*.[22] and Yoshikawa *et al*.[12] In the present work, we have developed a theory for NPLIN of KCl based on dielectric polarizability. The evidence for the Kerr-effect mechanism for NPLIN presented by Garetz and co-workers is not in question, and the operation of both mechanisms is entirely plausible. We believe that the dielectric polarizability may make an additional contribution at different power regimes to the effect observed by Garetz and co-workers: this could account for the more complex power dependence seen for urea.

In Fig. 6 we reproduce Fig. 1 but with the model curves, rather than heuristic straight-line fits. The model predicts that there is a zero threshold electric field required for nucleation, whereas the

experiments show that nucleation is not observed until the laser power is $6.4\ \mathrm{MW\ cm^{-2}}$. To match the experimental observations, the model power values have all been increased by the value of the threshold power. In addition, the model fractions *f* have been multiplied by the best fit-empirical scaling factor, *k*. Both the supersaturation and electric-field dependences of the model results match those in the experimental data very well (Figs. 5 and 6, respectively).

At the present time, we do not have an explanation for the apparent existence of the threshold power. Our model, based on classical nucleation theory, does not inform us about the microscopic mechanism of nucleation, i.e., how a cluster responds to the applied field. A cluster that becomes critical during the presence of the electric field pulse has no guarantee of survival once the field has gone. The true mechanism may depend either on some internal structural re-arrangement of the nucleus, or may depend on transport of additional KCl to the cluster. Experimental measurements of the diffusivity, $D = 2.1 \times 10^{-9}\ \mathrm{m^2\ s^{-1}}$, in saturated KCl give a root-mean-square estimate of the radius of diffusion $r_{rms} \sim 3.5\ \mathrm{nm\ ns^{-1}}$, which is not significantly different from the value in dilute solution.[28] At the saturation concentration there are $\rho = 1.6 \times 10^{28}$ cations per cubic metre, and the mean separation between ions, $\rho^{-1/3} = 4\text{Å}$. Therefore, the ions can travel many multiples of $\rho^{-1/3}$ during the 7 ns pulse duration. We have investigated the possibility that smaller clusters may not have the ability to attract sufficient KCl during the 7 ns of the pulse to permit survival after the pulse has ended. However, we find that this does not reproduce the distinct threshold: the probability of nucleation is still found to increase monotonically with power from $E = 0$. As for structure of the cluster, our model takes no account of the shortcomings of classical nucleation theory that have already been documented, such as the complex shapes, sizes, and qualities of crystal nuclei and the apparent size-dependent interfacial tensions between the crystal and the mother liquor.[29,30]

The best-fit value that we obtain for the interfacial tension $\gamma = 2.19 \pm 0.03\ \mathrm{mJ\ m^{-2}}$ (296.15 K) is in good agreement with previous results obtained from studies of 'homogeneous' nucleation rates in aqueous solutions: e.g., $\gamma = 2.80\ \mathrm{mJ\ m^{-2}}$ (303.2 K) of Preckshot and Brown,[31] $\gamma = 2.74\ \mathrm{mJ\ m^{-2}}$ (308.15 K) of Chatterji and Singh,[32] and $\gamma = 0.98\ \mathrm{mJ\ m^{-2}}$ (301.05 K) of Linnikov.[33] There has been considerable debate as to whether values of interfacial tension obtained from rate studies are too low as a result of heterogeneous nucleation on impurities or at surfaces. Moreover, the values depend on the theoretical model applied to the experimental nucleation-rate data.[34] Nielsen and Söhnel have re-calculated values of the interfacial tension using previously determined experimental induction times for a range of solutes, assuming mononuclear two-dimensional growth.[35] Their calculated best-value for KCl, $\gamma = 30\ \mathrm{mJ\ m^{-2}}$, was much larger than previous reports.

Using our best-fit interfacial tension $\gamma = 2.19 \pm 0.03$ mJ m^{-2} the classical nucleation model returns some absolute numerical values that are difficult to accept as being realistic. At supersaturation S = 1.050, we find that the critical radius in absence of the field is $r_c(0) = 1.37$ nm, with a classical barrier height $\Delta G(r,0) = 4.21 k_B T$ (296.15 K). At a peak power of 15 MW cm^{-2} (well above threshold), the electric field strength $E = 1.06 \times 10^7$ V m^{-1}, and we find that the dielectric free energy of the critical nucleus is only $\Delta W(E) = -5.32 \times 10^{-4}\, k_B T$. Moreover, the critical radius in the presence of the field $r_c(E)$ is reduced from $r_c(0)$ by a miniscule amount (10^{-4} nm). A larger value of interfacial tension $\gamma = 30$ mJ m^{-2} gives $r_c(0) = 18.8$ nm and an electrostatic value, $\Delta W(E) = -1.37 k_B T$, that is closer to $k_B T$; however, the classical barrier is considerably higher, $\Delta G(r,0) = 1.08 \times 10^4\, k_B T$. Clearly, the true NPLIN mechanism involves the exertion of a more significant influence than classical nucleation theory will allow.

The experimental observations might be rationalized to some extent by considering that the KCl grows on the surface of an impurity particle. In the present experiments these could be < 200 nm in size (due to filtration), or—less likely—some unexpected contamination. An impurity could essentially increase the magnitude of the electrostatic term without the energetic expense of growing massive clusters of KCl. An impurity could also modify the free-energy profile through the interfacial term: the area of nucleus that is in contact with the impurity is no longer in contact with the solution, and if the crystal–impurity interactions are favorable, this can lower the overall interfacial energy term.

With the observation of one crystal of KCl per shot within the current experimental conditions, it is worth noting that the laser induces nucleation by interaction with an exceedingly rare species. The above values suggest that to benefit from the electrostatic energy, such species should be quite large (r > 20 nm). Whether these species are homogeneous or heterogeneous in composition is not yet clear. In spite of this, we have demonstrated that a simple modified classical nucleation model adequately reproduces the electric field and supersaturation dependences of the observed nucleation. Further experiments are underway to elucidate the laser-induced nucleation mechanism for the alkali halides.

5. Conclusions

In summary, we have made quantitative measurements of the non-photochemical laser-induced nucleation of supersaturated aqueous potassium chloride. We have shown that the likely mechanism

for the effect involves the isotropic electronic polarization of sub-critical KCl clusters by the laser light, and a modified free-energy surface on which a small proportion of the clusters become supercritical. Calculations using a classical nucleation theory provide excellent descriptions of the crystallization yield as a function of both laser power and supersaturation. Fitting this theory to the experimental results gave a phenomenological value of the crystal-solution interfacial tension of $\gamma = 2.19 \pm 0.03 \text{ mJ m}^{-2}$.

Our theoretical model is capable of fitting the observed experimental data; however, there are details of the laser-induced nucleation mechanism that are still unclear. The experiments have shown that it is possible to nucleate a single crystal of KCl almost on demand (within the ns pulse width). Therefore, we believe the method shows tremendous promise for unraveling the first moments during the birth of a crystal nucleus.

Figures

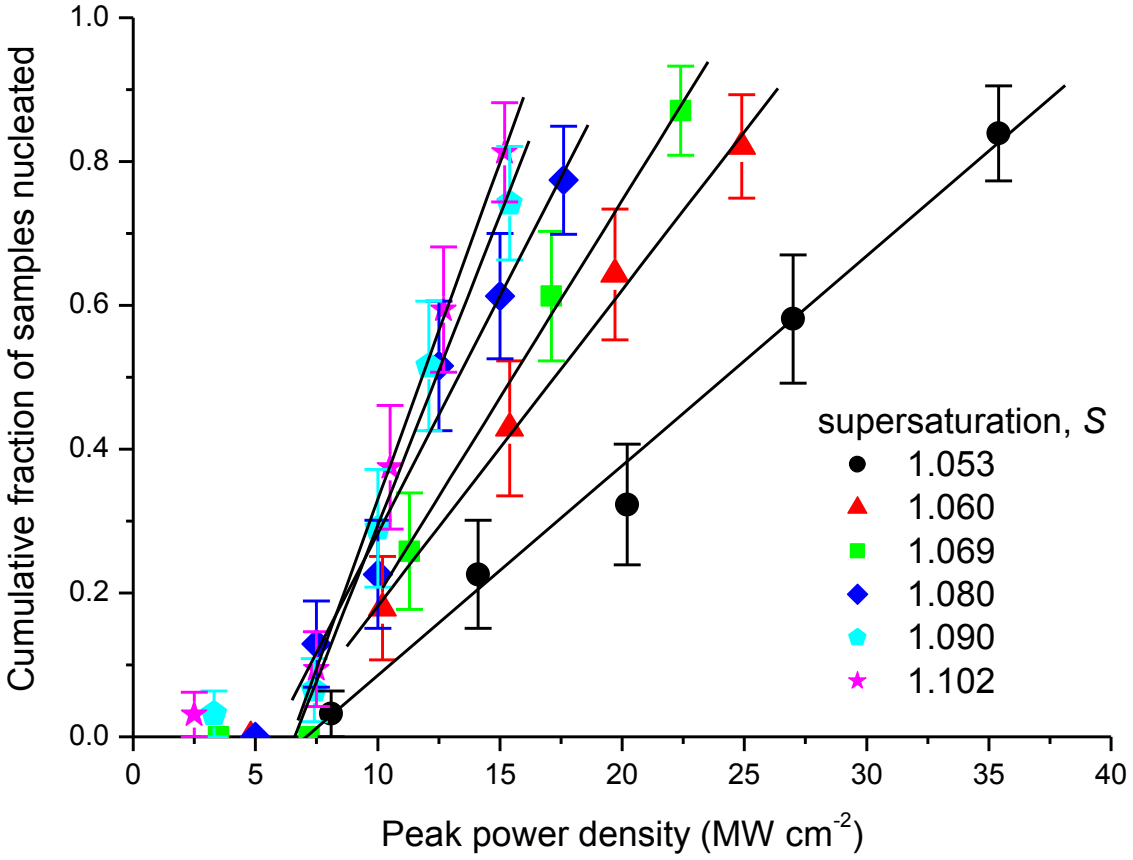

Fig. 1. Plots of the fraction of samples nucleated versus the peak power density. Points represent experimental results at different values of supersaturation, $S = 1.053$ (circles), 1.060 (triangles), 1.069 (squares), 1.080 (diamonds), 1.090 (pentagons), 1.102 (stars). The lines were obtained by least-squares fitting of the experimental data for each supersaturation. The experimental data show a threshold power density value of $6.4 \pm 0.5\,\mathrm{MW\,cm^{-2}}$. The slope of the plot is a measure of how *labile* the samples are to nucleation at a given supersaturation, which we refer to as the *lability* of the sample (see text for details).

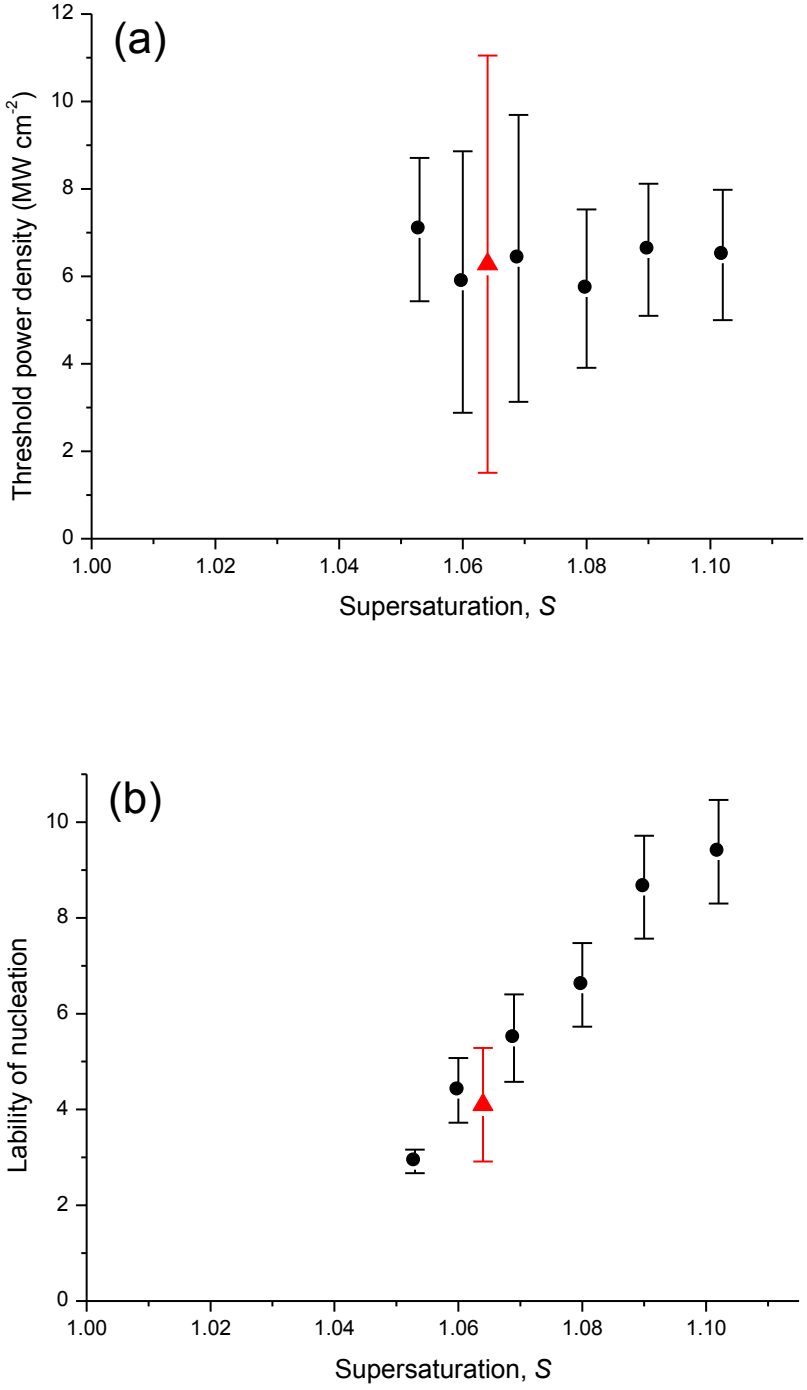

Fig. 2. (a) Plot of threshold peak power density versus supersaturation, S at $23\,^{\circ}\mathrm{C}$. (b) Plot of the nucleation power-dependence or lability (obtained as the slopes in Fig. 1) versus supersaturation, S. Also shown are results obtained using high purity samples and clean preparation (red triangle): see text for details.

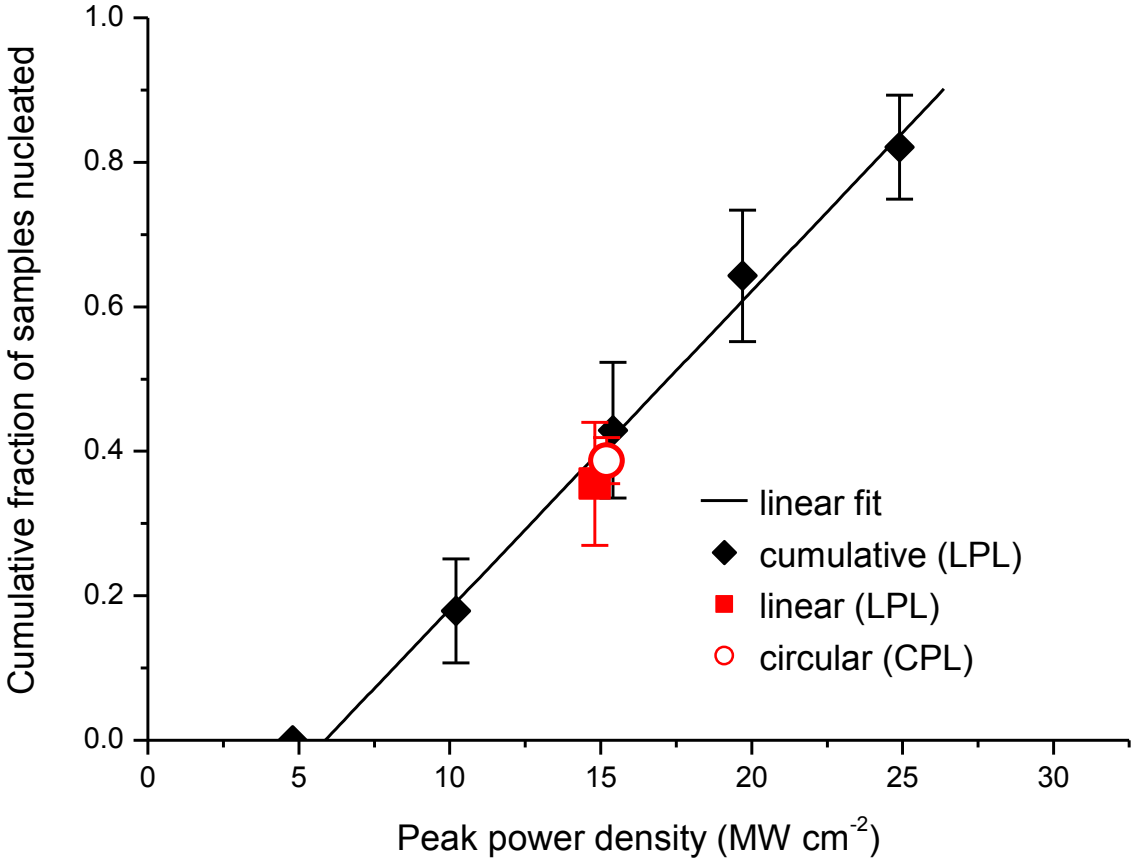

Fig. 3. Plot of fraction of samples nucleated versus peak power density, for $S = 1.060$, illustrating the lack of dependence of nucleation on polarization of the laser light. Diamonds and the straight line are the cumulative experimental points (linearly polarized light) and fit, respectively, taken from Fig. 1. The other points show the results for all samples being shot at peak power density $15\ \mathrm{MW\ cm^{-2}}$ with linearly polarized light (square) and circularly polarized light (circle): the two points have been plotted offset in power slightly to enable comparison.

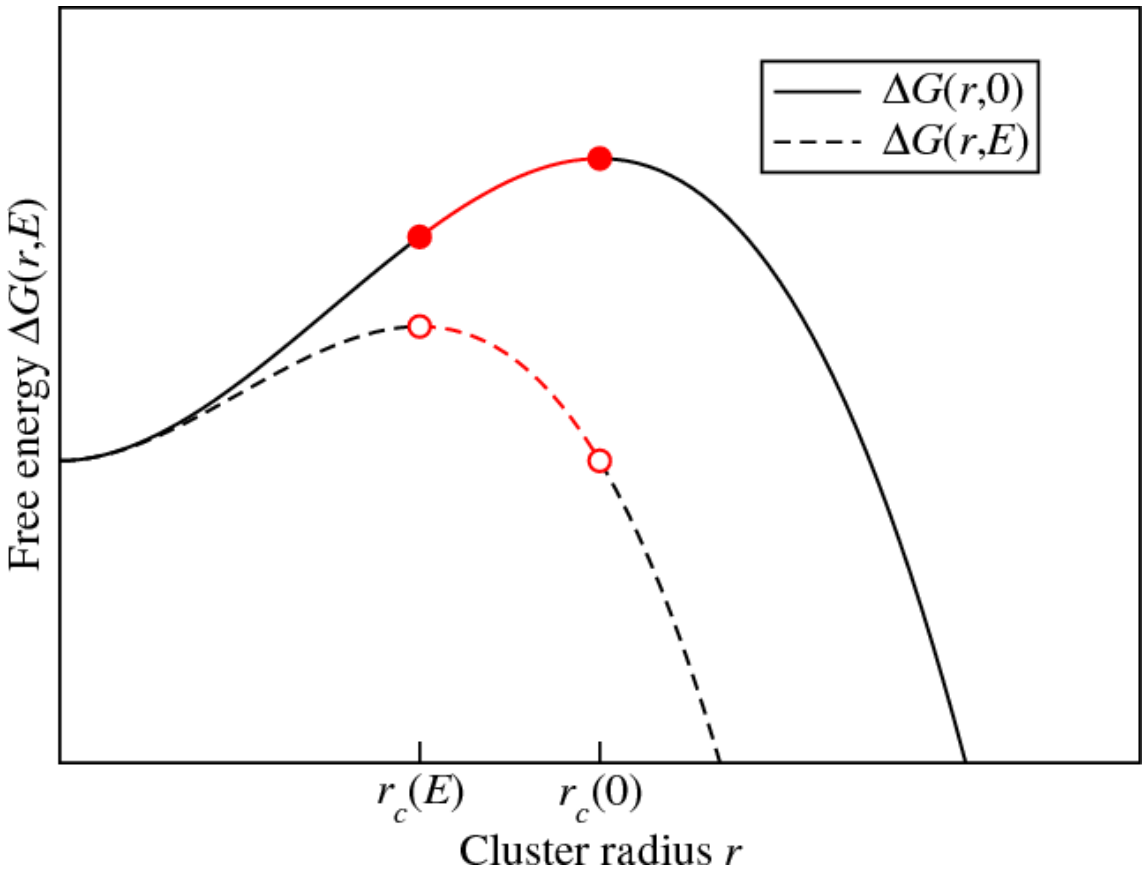

Fig. 4. Schematic free-energy curves, showing the dependence of the critical cluster radius and the barrier height on the electric field strength. Upon the application of an electric field, clusters with radii in the range $r_c(E) \le r \le r_c(0)$ (indicated in red, and initially subcritical) will become supercritical and hence be liable to nucleate.

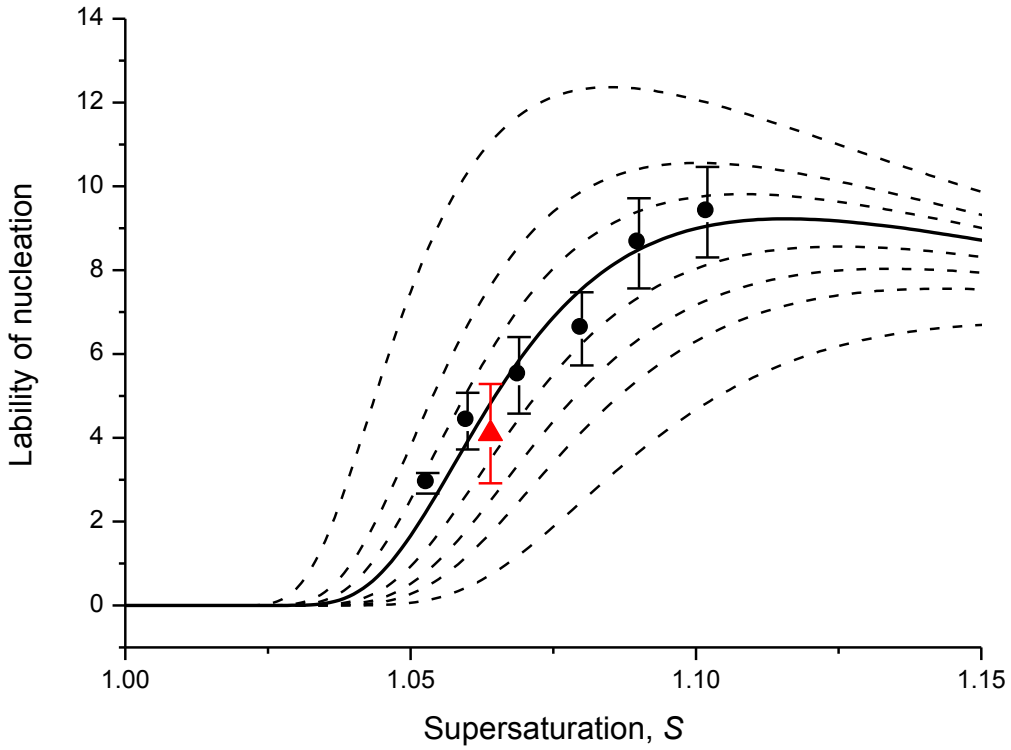

Fig. 5. Plot of the lability of nucleation versus supersaturation, *S*. Experimental results (from Fig. 2b) are shown as solid symbols and model results as lines. The model curves shown are for values of the surface energy γ = 2.7, 2.5, 2.4, 2.3, 2.19, 2.1, 2.0, 1.8 mJ m^{-2} from lowest curve to highest, respectively. The curve corresponding to the best-fit value of the interfacial tension $\gamma = 2.19 \pm 0.03$ mJ m^{-2} is shown as the solid line. All model results have been scaled by the best-fit scaling parameter $k = (7.78 \pm 0.12) \times 10^4$.

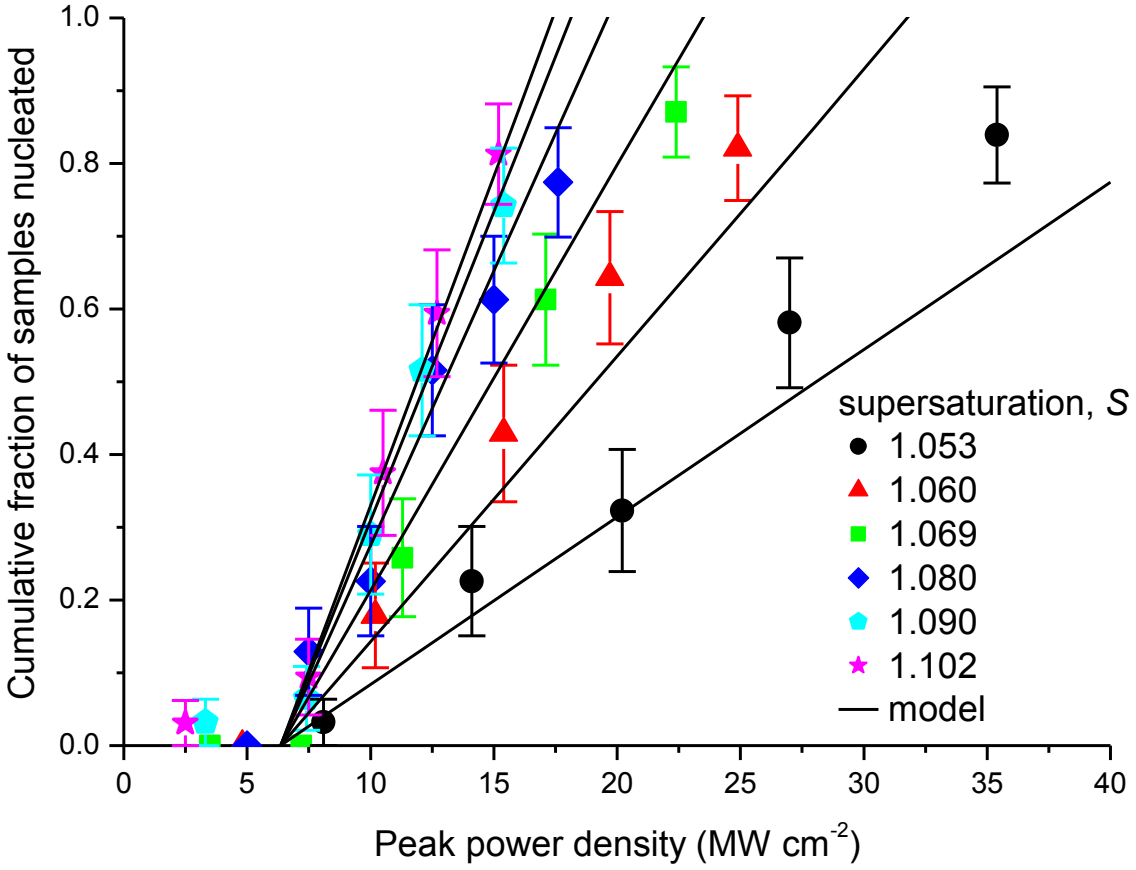

Fig. 6. Plots of the fraction of samples nucleated versus the peak power density, *cf.* Fig. 1. Points represent experimental results, at different values of supersaturation, $S = 1.053$ (circles), 1.060 (triangles), 1.069 (squares), 1.080 (diamonds), 1.090 (pentagons), 1.102 (stars). The lines were obtained from the model using the best-fit values of the surface energy $\gamma = 2.19 \pm 0.03$ mJ m^{-2} and scaling parameter $k = (7.78 \pm 0.12) \times 10^4$ determined from the best fit shown in Fig. 5. The model values have been shifted along the power axis (horizontal axis) to match the experimentally determined threshold value of $6.4\,\mathrm{MW\,cm^{-2}}$.

References

(1) Tyndall, J. *Phil. Mag.* **1869**, *37*, 384.

(2) Tam, A.; Moe, G.; Happer, W. *Phys. Rev. Lett.* **1975**, *35*, 1630.

(3) Okutsu, T.; Nakamura, K.; Haneda, H.; Hiratsuka, H. *J. Cryst. Growth* **2004**, *4*, 113.

(4) Adachi, H.; Takano, K.; Hosokawa, Y.; Inoue, T.; Mori, Y.; Matsumura, H.; Yoshimura, M.; Tsunaka, Y.; Morikawa, M.; Kanaya, S.; Masuhara, H.; Kai, Y.; Sasaki, T. *Jap. J. Appl. Phys.* **2003**, *42*, L798.

(5) Garetz, B. A.; Aber, J. E.; Goddard, N. L.; Young, R. G.; Myerson, A. S. *Phys. Rev. Lett.* **1996**, *77*, 3475.

(6) Boyd, R. W. *Nonlinear optics*; 2nd ed.; Academic Press: San Diego, CA, 2003.

(7) Garetz, B. A.; Matic, J.; Myerson, A. S. *Phys. Rev. Lett.* **2002**, *89*, 175501.

(8) Zaccaro, J.; Matic, J.; Myerson, A. S.; Garetz, B. A. *Cryst. Growth Des.* **2001**, *1*, 5.

(9) Sakai, H.; Hosogai, H.; Kawakita, T.; Onuma, K.; Tsukamoto, K. *J. Cryst. Growth* **1992**, *116*, 421.

(10) Sun, X.; Garetz, B. A.; Myerson, A. S. *Cryst. Growth Des.* **2008**, *8*, 1720.

(11) Sun, X. Y.; Garetz, B. A.; Myerson, A. S. *Cryst. Growth Des.* **2006**, *6*, 684.

(12) Yoshikawa, H. Y.; Hosokawa, Y.; Masuhara, H. *Jap. J. Appl. Phys.* **2006**, *45*, L23.

(13) Nakamura, K.; Hosokawa, Y.; Masuhara, H. *Cryst. Growth Des.* **2007**, *7*, 885.

(14) Sugiyama, T.; Adachi, H.; Masuhara, H. *Chem. Lett.* **2007**, *36*, 1480.

(15) Khamskii, E. V. *Crystallization from solutions*; Consultants Bureau: New York, 1969.

(16) Cheremisin, A. I. *Izv. Vyssh. Uchebn. Zaved. Fiz.* **1970**, *13*, 129.

(17) Kaschiev, D. *J. Cryst. Growth* **1972**, *13/14*, 128.

(18) Isard, J. O. *Phil. Mag.* **1977**, *35*, 817.

(19) Taleb, M.; Didierjean, C.; Jelsch, C.; Mangeot, J. P.; Capelle, B.; Aubry, A. *J. Cryst. Growth* **1999**, *200*, 575.

(20) Penkova, A.; Gliko, O.; Dimitrov, I. L.; Hodjaoglu, F. V.; Nanev, C.; Vekilov, P. G. *J. Cryst. Growth* **2005**, *275*, e1527.

(21) Aber, J. E.; Arnold, S.; Garetz, B. A.; Myerson, A. S. *Phys. Rev. Lett.* **2005**, *94*, 3475.

(22) Matic, J.; Sun, X. Y.; Garetz, B. A.; Myerson, A. S. *Cryst. Growth Des.* **2005**, *5*, 1565.

(23) Fröhlich, H. *Theory of dielectrics: dielectric constant and dielectric loss*; Clarendon Press: Oxford, 1958.

(24) Warshavsky, V. B.; Shchekin, A. K. *Colloids And Surfaces A* **1999**, *148*, 283.

(25) In *Handbook of Chemistry and Physics*; 88th ed.; Lide, D. R., Ed.; CRC Press: Boca Raton, FL, 2007.

(26) Frenkel, J. *The kinetic theory of liquids*; Dover: New York, 1955.

(27) Mullin, J. W. *Crystallization*; 4th ed.; Butterworth-Heinemann: Oxford, 2001.

(28) Chang, Y. C.; Myerson, A. S. *AiChE Journal* **1985**, *31*, 890.

(29) Moroni, D.; ten Wolde, P. R.; Bolhuis, P. G. *Phys. Rev. Lett.* **2005**, *94*, 235703.

(30) Zykova-Timan, T.; Valeriani, C.; Sanz, E.; Frenkel, D.; Tosatti, E. *Phys. Rev. Lett.* **2008**, *100*, 036103.

(31) Preckshot, G. W.; Brown, G. G. *Ind. Eng. Chem.* **1952**, *44*, 1314.

(32) Chatterji, A. C.; Singh, R. N. *J. Phys. Chem.* **1958**, *62*, 1408.

(33) Linnikov, O. D. *Cryst. Res. Technol.* **2004**, *39*, 529.

(34) Wu, W. J.; Nancollas, G. H. *Adv. Colloid Interface Sci.* **1999**, *79*, 229.

(35) Nielsen, A. E.; Söhnel, O. *J. Cryst. Growth* **1971**, *11*, 233.